

Magnetoresistance of $\text{Pr}_{1-x}\text{La}_x\text{Os}_4\text{Sb}_{12}$: Disentangling local crystalline-electric-field physics and lattice effects

C. R. Rotundu, K. Ingersent, and B. Andraka*

Department of Physics, University of Florida P.O. Box 118440, Gainesville, Florida 32611-8440, USA

(Dated: August 13, 2018)

Resistivity measurements were performed on $\text{Pr}_{1-x}\text{La}_x\text{Os}_4\text{Sb}_{12}$ single crystals at temperatures down to 20 mK and in fields up to 18 T. The results for dilute-Pr samples ($x = 0.3$ and 0.67) are consistent with model calculations performed assuming a singlet crystalline-electric-field (CEF) ground state. The residual resistivity of these crystals features a smeared step centered around 9 T, the predicted crossing field for the lowest CEF levels. The CEF contribution to the magnetoresistance has a weaker-than-calculated dependence on the field direction, suggesting that interactions omitted from the CEF model lead to avoided crossing in the effective levels of the Pr^{3+} ion. The dome-shaped magnetoresistance observed for $x = 0$ and 0.05 cannot be reproduced by the CEF model, and likely results from fluctuations in the field-induced antiferroquadrupolar phase.

PACS numbers: 74.25.Ha, 74.70.Tx

I. INTRODUCTION

$\text{PrOs}_4\text{Sb}_{12}$, the first discovered Pr-based heavy fermion and superconductor,¹ remains a focus of extensive theoretical and experimental investigation. Its significance lies in the fact that the origin of the heavy-fermion behavior is associated with non-Kramers f -electron ions, for which the conventional Kondo effect seems unlikely. Our previous specific-heat results in magnetic fields² established that the crystalline-electric-field (CEF) ground state is a nonmagnetic Γ_1 singlet. The field dependence of the CEF Schottky anomaly for fields greater than 14 T is clearly inconsistent with the alternative scenario of a nonmagnetic Γ_3 doublet ground state. This conclusion was independent of whether the exact T_h point-group symmetry or the higher (approximate) O_h symmetry was assumed for the Pr sites.³ The singlet nature of the CEF ground state was subsequently confirmed by inelastic neutron scattering measurements and their analysis within the T_h symmetry scheme.⁴

Despite the overwhelming evidence in favor of a singlet CEF ground state, there are experimental results for $\text{PrOs}_4\text{Sb}_{12}$ that seem to be better understood in terms of a doublet ground state. For example, the magnetoresistance^{1,5,6,7} at 1.4 K exhibits a dome-like shape that is consistent with model calculations of the CEF resistivity for a Γ_3 ground state and inconsistent with similar calculations for a Γ_1 ground state.⁵ However, the CEF resistivity is a single-ion property that might be strongly affected in $\text{PrOs}_4\text{Sb}_{12}$ by lattice coherence and by strong quadrupolar and exchange interactions. To probe this possibility, we have performed magnetoresistance measurements on single-crystal $\text{Pr}_{1-x}\text{La}_x\text{Os}_4\text{Sb}_{12}$, in which lattice translational symmetry is broken and intersite effects should be weaker than in the pure compound. Based on previously published magnetic susceptibility and specific heat results,⁸ we do not expect significant changes in CEF energies (and eigenstates) of Pr upon doping with La. In addition, we have extended magnetoresistance measurements of the undoped mate-

rial down to 20 mK.

We find that the magnetoresistance of pure $\text{PrOs}_4\text{Sb}_{12}$ at 20 mK is inconsistent with model calculations for either the Γ_3 or the Γ_1 CEF ground state, and conclude that the dome feature most probably results from fluctuations in the field-induced antiferroquadrupolar (AFQ) phase. On dilution of the Pr lattice with La, the dome in the magnetoresistance is replaced by a smeared step that is consistent with the picture of a Γ_1 singlet CEF ground state but not with a Γ_3 doublet. The dependence of the f -electron contribution to the magnetoresistance on the direction of the magnetic field is smaller than is predicted theoretically based on a CEF model. This discrepancy suggests that interactions omitted from the CEF model lead to avoided crossing in the effective levels of the Pr^{3+} ion.

II. METHODS

Results are presented below for $\text{Pr}_{1-x}\text{La}_x\text{Os}_4\text{Sb}_{12}$ with four different La concentrations: $x = 0, 0.05, 0.3,$ and 0.67 . For $x = 0, 0.3,$ and 0.67 , we grew large single crystals (cubes with masses as large as 50 mg) on which accurate magnetic susceptibility measurements were performed up to 300 K in order to extract the room-temperature paramagnetic effective moment. In each case, this moment was within 10% of that expected for Pr^{3+} . (For the undoped compound, this finding contradicts a wide range of values reported in literature.) The superconducting transition temperatures T_c of the large single crystals and of smaller resistivity bars, also obtained in the same growths, were checked via ac susceptibility measurements. A good agreement between T_c values of large and small crystals confirmed the stoichiometry assigned to samples used in this study. The residual resistivity ratio (the ratio of the resistance at room temperature to that extrapolated to $T = 0$) was $\text{RRR} = 100, 50, 180,$ and 170 for $x = 0, 0.05, 0.3,$ and 0.7 , respectively. The value $\text{RRR} = 100$ exceeds those re-

ported previously^{1,7,9} for pure $\text{PrOs}_4\text{Sb}_{12}$, indicative of the high quality of our samples. The $x = 0.05$ crystal was from the batch for which results were reported in Ref. 8.

The resistivity was measured by a conventional four-probe technique. The estimated uncertainty in the determination of the absolute value of the resistivity was 30% due to the unfavorable geometry of the crystals. Within this uncertainty, the resistivity at room temperature was the same in all cases. In the plots below, we have scaled the resistivity of each sample to a zero-field room-temperature value of $300 \mu\Omega\text{cm}$, in the range reported previously. It is important to emphasize that this scaling procedure is in no way essential for the conclusions of the paper, which are based on the temperature and field dependence of the resistivity of a given sample.

We calculated the CEF contribution ρ_{CEF} to the electrical resistivity via the method applied by Fisk and Johnston¹⁰ to the resistivity of PrB_6 and by Frederick and Maple⁵ to the magnetoresistance of $\text{PrOs}_4\text{Sb}_{12}$. This method focuses on a single Pr ion, neglects intersite effects, and takes no account of the direction of the current relative to the crystal axes or to the magnetic field. Our calculations started with one or other of two forms for \hat{H}_0 , the CEF Hamiltonian for Pr^{3+} in zero magnetic field: that (corresponding in the O_h -symmetry notation of Ref. 11 to $W = -2.97 \text{ K}$ and $x = -0.7225$) deduced⁵ by fitting the temperature dependence of the zero-field resistivity of $\text{PrOs}_4\text{Sb}_{12}$; or the Hamiltonian (described in the T_h -symmetry notation of Ref. 3 by $W = 3.0877 \text{ K}$, $x = 0.45991$, and $y = 0.10503$) determined from elastic¹² and inelastic⁴ neutron scattering. Henceforth, we refer to these cases as the “doublet” and “singlet” CEF scheme, respectively, according to the ground-state degeneracy of \hat{H}_0 .

The CEF states in a magnetic field \mathbf{H} were obtained by diagonalizing the Hamiltonian $\hat{H}_0 + g\mu_B\mathbf{H} \cdot \hat{\mathbf{J}}$, where $g = 4/5$ is the Landé g factor for Pr^{3+} and $\hat{\mathbf{J}}$ is the f -electron angular momentum operator. The CEF resistivity is completely determined by these CEF states, the temperature T , and two constants ρ_{ex} and ρ_A , which parametrize, respectively, the overall strengths of magnetic exchange and the aspherical Coulomb interaction between the $4f$ and conduction electrons. Following Ref. 5, we took $\rho_{\text{ex}} = \rho_A = 0.25 \mu\Omega\text{cm}$. However, our conclusions are insensitive to the particular choice of constants.

III. RESULTS AND DISCUSSION

Figure 1 shows the resistivity of undoped $\text{PrOs}_4\text{Sb}_{12}$ for three representative fields, with both current and magnetic field oriented along the (001) direction. The results are similar to those reported by other groups.^{1,13} Below 200–300 mK the resistivity saturates but has a strong field variation. The residual resistivity ρ_0 can be obtained using the previously noted^{1,13} temperature variation at fixed field: $\rho(T) = \rho_0 + BT^n$ with $n > 2$. Within the precision of our measurement, there is no difference

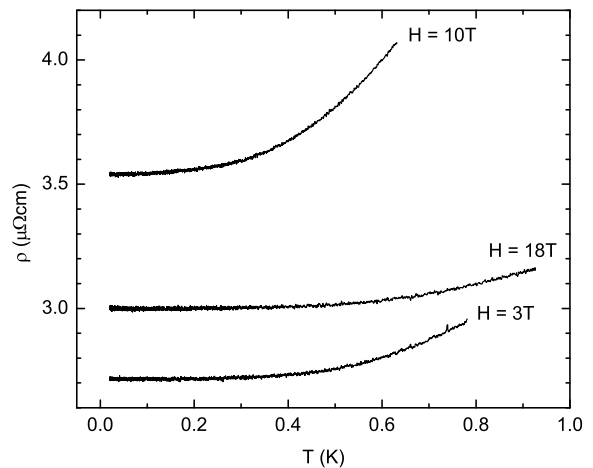


FIG. 1: Resistivity vs temperature for $\text{PrOs}_4\text{Sb}_{12}$ in three different magnetic fields, with both current and field along the (001) direction.

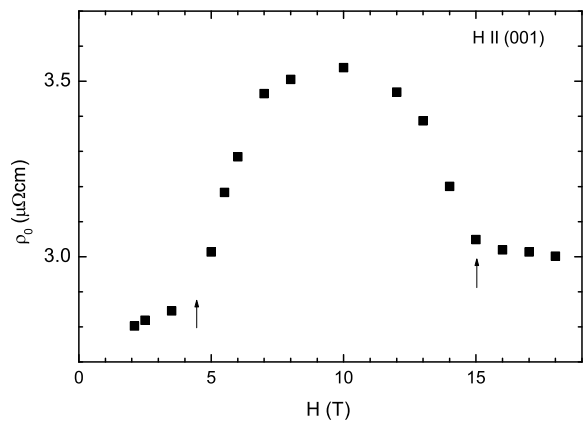


FIG. 2: Residual resistivity vs magnetic field for $\text{PrOs}_4\text{Sb}_{12}$, with both current and field along the (001) direction. Arrows indicate boundaries between paramagnetic and field-induced ordered phases.

between ρ_0 obtained in this manner and $\rho(T = 20 \text{ mK})$.

This residual resistivity (or resistivity at 20 mK), when plotted against magnetic field (Fig. 2), has a dome shape centered around 9–10 T. Such a dome-shaped magnetoresistance has been reported previously at the somewhat higher temperatures of 1.4 K (Ref. 5) and 0.36 K (Ref. 7). Two explanations for this dome have been considered: field-induced long-range antiferroquadrupolar (AFQ) order, and crossing of the lowest CEF levels. It is striking that $\rho_0(H)$ rises sharply at the AFQ boundaries, indicated by arrows in Fig. 2, and peaks around 10 T, where the AFQ transition temperature is highest. However, Frederick and Maple have shown (see Fig. 2 of Ref. 5) that the width, peak position, and height of the dome in the magnetoresistance of $\text{PrOs}_4\text{Sb}_{12}$ at 1.4 K are reproduced quite well by the single-ion CEF resistivity computed within the doublet scheme. (By contrast, ρ_{CEF} for the singlet scheme shows a step-like increase in the vicin-

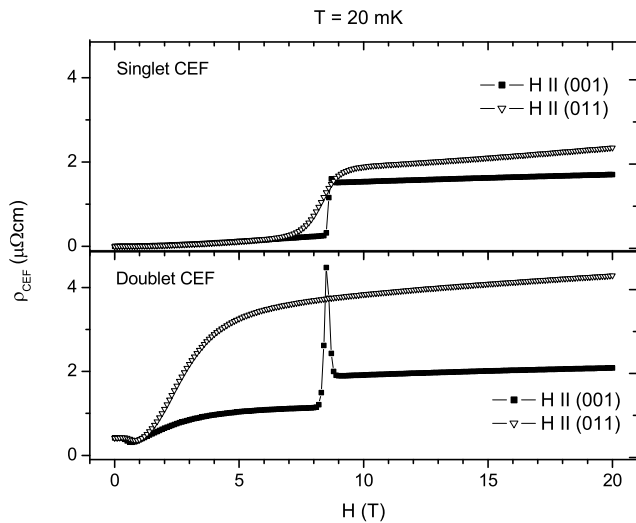


FIG. 3: Theoretical CEF resistivity at 20 mK vs magnetic field calculated within the singlet (upper panel) and doublet (lower panel) CEF schemes, for fields along (001) (■) and (011) (▽).

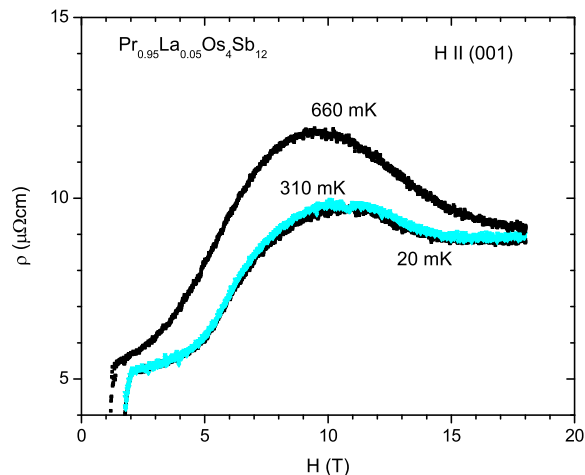


FIG. 4: (color online) Longitudinal magnetoresistance of $\text{Pr}_{0.95}\text{La}_{0.05}\text{Os}_4\text{Sb}_{12}$ at 20, 310, and 660 mK, for current and field along the (001) direction.

ity of the crossing field at which the lowest $T_h \Gamma_4^{(2)}$ level falls in energy below the Γ_1 singlet.)

We find that neither CEF scheme accounts satisfactorily for the magnetoresistance measured at 20 mK (Fig. 2), which shows a dome of similar width to that at 1.4 K. Irrespective of the CEF scheme, ρ_{CEF} for fields oriented along the (001) direction (square symbols in Fig. 3) is discontinuous at the crossing field and essentially flat at higher fields. It therefore seems that the low-temperature magnetoresistance of $\text{PrOs}_4\text{Sb}_{12}$ is dominated by effects beyond those considered in the single-ion CEF model.

We now turn to the effects of La doping. Figure 4 shows the magnetoresistance of $\text{Pr}_{0.95}\text{La}_{0.05}\text{Os}_4\text{Sb}_{12}$ at 20, 310, and 660 mK. Similarly to $\text{PrOs}_4\text{Sb}_{12}$, there is

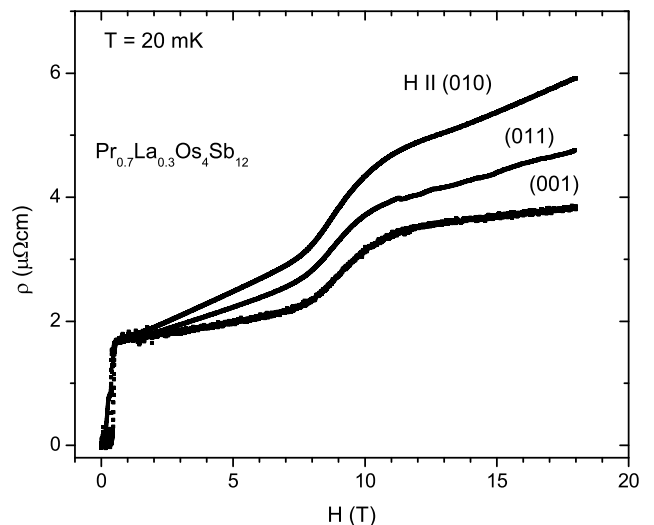


FIG. 5: Magnetoresistance of $\text{Pr}_{0.7}\text{La}_{0.3}\text{Os}_4\text{Sb}_{12}$ at 20 mK for three different orientations of the magnetic field. The current direction was (001).

a negligible temperature variation of the resistivity below 300 mK in fields above-critical for superconductivity (as evidenced by the overlap of the 20-mK and 310-mK isotherms). However, the shape of the dome for $x = 0.05$ is much less symmetric about the peak field than its $x = 0$ counterpart. Between 2 T and 10 T, $\rho(T=20 \text{ mK})$ for the doped sample increases by over 80%, compared to a 25% increase for the undoped material, whereas the resistivity drop above 10 T is greater in percentage terms for $x = 0$.

The magnetoresistance becomes qualitatively different at higher La doping. Figure 5 shows the 20-mK magnetoresistance of $\text{Pr}_{0.7}\text{La}_{0.3}\text{Os}_4\text{Sb}_{12}$ for fields along (001), (011), and (010); in each case, the current passed along the (001) direction. All three isotherms exhibit a pronounced but wide step, centered near 9–10 T, superimposed on a linear background. In the investigated field range this $x = 0.3$ material does not exhibit the dome structure characteristic of $x = 0$ and 0.05. For each curve, ρ versus H is approximately linear above 13 T. The resistivity of the non- f -electron analog $\text{LaOs}_4\text{Sb}_{12}$, measured at 0.36 K, has a quite large and approximately linear field dependence.⁷ Furthermore, the directional dependence of the magnetoresistance of $\text{LaOs}_4\text{Sb}_{12}$ — $d\rho/dH$ being larger along (011) than along (001)—is in agreement with the trend of the linear background in Fig. 5. It thus seems that the differences between the high-field slopes of $\rho(H)$ in Fig. 5 can be attributed primarily to non- f -electron contributions to the magnetoresistance. Subtracting such linear parts results in very similar curves (not shown) for all three field directions. We conclude that the f -electron magnetoresistance in this moderately doped material is nearly isotropic.

Compared to the cases $x = 0$ and $x = 0.05$, the low-temperature magnetoresistance of $\text{Pr}_{0.7}\text{La}_{0.3}\text{Os}_4\text{Sb}_{12}$ for fields along (001) is much closer to that given by the CEF

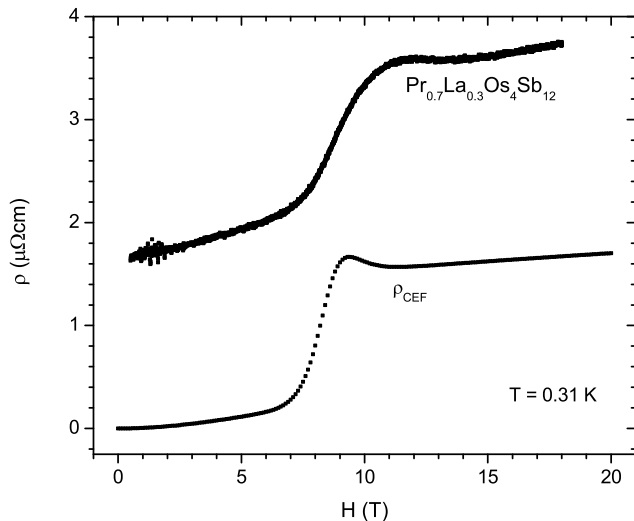


FIG. 6: Measured magnetoresistance of $\text{Pr}_{0.7}\text{La}_{0.3}\text{Os}_4\text{Sb}_{12}$ at 310 mK for current and field along the (001) direction, and theoretical CEF resistivity ρ_{CEF} for the same temperature and field direction.

model. The 20-mK measurements (Fig. 5) are more consistent with the singlet CEF scheme than with the doublet scheme, in that the latter predicts a sharp peak that is absent in the data. A second and stronger argument in favor of the singlet scheme is provided by the near-isotropy of the f -electron magnetoresistance noted in the previous paragraph. Figure 3 plots the CEF resistivity for fields along (001) and (011). The doublet scheme (lower panel in Fig. 3) predicts a highly anisotropic ρ_{CEF} stemming from the fact that the lowest two CEF levels cross at 8.5 T along (001), but instead diverge along (011). In the singlet CEF scheme (upper panel in Fig. 3), the anisotropy is much smaller because the lowest CEF levels cross at 8.6 T along (001), while along the (011) direction they anticross at 8.3 T with a minimum gap of only 0.7 K. Unlike the doublet CEF scheme, the singlet scheme does a reasonable job of reproducing the measured (011) magnetoresistance. However, it underestimates the width of the step for fields along (001), and hence still overestimates the anisotropy in the f -electron magnetoresistance extracted from Fig. 5.

Figure 6 shows that at the higher temperature of 310 mK, there is much better agreement between the magnetoresistance of $\text{Pr}_{0.7}\text{La}_{0.3}\text{Os}_4\text{Sb}_{12}$ along (001) and ρ_{CEF} calculated within the singlet CEF scheme. At this temperature, the thermal smearing of the step in ρ_{CEF} matches quite well the width of the rise in the measured magnetoresistance. The results of similar calculations for the doublet scheme (not shown, but very similar to the 350-mK results in Fig. 2 of Ref. 5) are in gross disagreement with the measurement.

The character of the magnetoresistance seems to be little changed by further La dilution. The longitudinal magnetoresistance for $x = 0.67$ was investigated down to 0.35 K and in fields to 14 T. The magnetoresistance at the

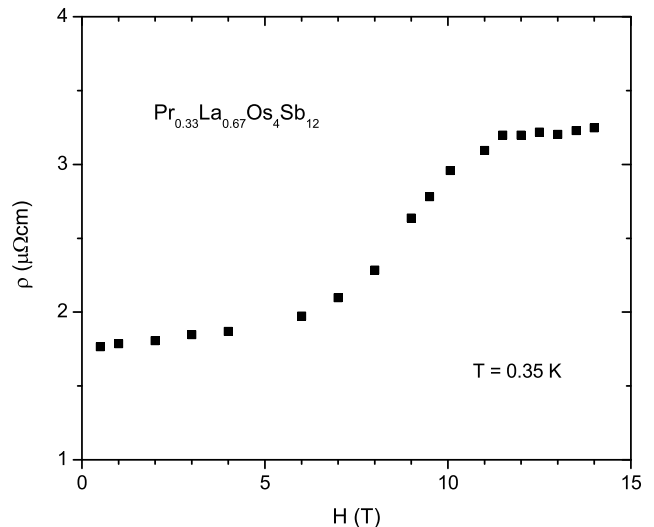


FIG. 7: Magnetoresistance of $\text{Pr}_{0.33}\text{La}_{0.67}\text{Os}_4\text{Sb}_{12}$ at 350 mK for current and field along the (001) direction.

lowest temperature (Fig. 7) exhibits essentially identical magnetic field dependence to that for $x = 0.3$.

The main difference between the f -electron magnetoresistance inferred for dilute-Pr alloys and that calculated in the singlet CEF scheme relates to the low-temperature width of the step along the (001) field direction. The CEF model predicts an almost discontinuous jump of the magnetoresistance at 20 mK at the level-crossing field, while the rise in the measured magnetoresistance of $\text{Pr}_{0.7}\text{La}_{0.3}\text{Os}_4\text{Sb}_{12}$ takes place over 3–4 T. Since there is better agreement between the measured and theoretical magnetoresistance along the (011) direction, where level anticrossing is expected, we speculate that interactions omitted from the CEF model mix the lowest levels, preventing any crossing even along high-symmetry field directions and thereby producing isotropic magnetoresistance. These interactions are most likely nonlocal. We note, however, that a mean-field treatment of intersite magnetic and quadrupolar interactions between Pr ions did not find avoided crossing.^{2,12}

Figure 6 shows that the measured midpoint field for the magnetoresistance rise in $\text{Pr}_{0.7}\text{La}_{0.3}\text{Os}_4\text{Sb}_{12}$ is about 1 T higher than is predicted based on the CEF level scheme determined for pure $\text{PrOs}_4\text{Sb}_{12}$. This perhaps points to a small shift in the CEF levels upon doping to 30% La. The similarity between the magnetoresistance steps observed for $x = 0.3$ and 0.67 suggests that there is little further evolution of the CEF energies over this doping range. A weak dependence of CEF levels on La doping is in agreement with our specific-heat measurements of the Schottky anomaly in lightly doped alloys,¹⁴ and is also supported by the nearly invariant temperature of the maximum in the magnetic susceptibility.⁸

The contrast between the resistivity versus field curves for the $x = 0$ and $x = 0.3$ samples is striking. The obvious differences between these two compositions are the

presence of a field-induced ordered phase for the pure material and the absence of translational symmetry in the diluted case. Our previous specific heat measurements¹⁴ indicate that the field-induced ordered (AFQ) phase disappears somewhere near $x = 0.2$. Since the model for the CEF resistivity are single-site in character, it seems likely that the dome-shaped magnetoresistance observed for $x = 0$ and 0.05 is associated with the presence of long-range order in these materials, perhaps through enhanced scattering of conduction electrons caused by fluctuations in the AFQ order parameter.

In summary, we have shown that a simple CEF model accounts quite well for the f -electron contribution to the magnetoresistance of $\text{Pr}_{1-x}\text{La}_x\text{Os}_4\text{Sb}_{12}$ with $x = 0.3$ and 0.67 . The weak dependence of this contribution on field direction is consistent with the existence of a singlet CEF in zero magnetic field, with avoided level crossing in ap-

plied fields. At the lowest temperatures, the magnetoresistance for $x = 0$ and $x = 0.05$ is inconsistent with the results of CEF model calculations. This discrepancy is attributed to the long-range order present in the pure and lightly doped materials.

Acknowledgments

Stimulating discussions with P. Kumar are acknowledged. This work has been supported by U.S. Department of Energy (DOE) Grant No. DE-FG02-99ER45748, by National Science Foundation (NSF) Grant No. DMR-0312939, and by the National High Magnetic Field Laboratory.

* Electronic address: andraka@phys.ufl.edu

¹ E. D. Bauer, N. A. Frederick, P.-C. Ho, V. S. Zapf, and M. B. Maple, Phys. Rev. B **65**, 100506(R) (2002).

² C. R. Rotundu, H. Tsujii, Y. Takano, B. Andraka, H. Sugawara, Y. Aoki, and H. Sato, Phys. Rev. Lett. **92**, 037203 (2004).

³ K. Takegahara, H. Harima, and A. Yanase, J. Phys. Soc. Jpn. **70**, 1190 (2001).

⁴ E. A. Goremychkin, R. Osborn, E. D. Bauer, M. B. Maple, N. A. Frederick, W. M. Yuhasz, F. M. Woodward, and J. W. Lynn, Phys. Rev. Lett. **93**, 157003 (2004).

⁵ N. A. Frederick and M. B. Maple, J. Phys.: Condens. Matter **15**, 4789 (2003).

⁶ P.-C. Ho, N. A. Frederick, V. S. Zapf, E. D. Bauer, T. D. Do, M. B. Maple, A. D. Christianson, and A. H. Lacerda, Phys. Rev. B **67**, 180508(R) (2003).

⁷ H. Sugawara, S. Osaki, E. Kuramochi, M. Kobayashi, S. R. Saha, T. Namiki, Y. Aoki, and H. Sato, Phys. Rev. B **72**, 014519 (2005).

⁸ C. R. Rotundu, P. Kumar, and B. Andraka, Phys. Rev. B

73, 014515 (2006).

⁹ H. Sugawara, S. Osaki, S. R. Saha, Y. Aoki, H. Sato, Y. Inada, H. Shishido, R. Settai, Y. Onuki, H. Harima, and K. Oikawa, Phys. Rev. B **66**, 220504(R) (2002).

¹⁰ Z. Fisk and D. C. Johnston, Solid State Commun. **22**, 359 (1977).

¹¹ K. R. Lea, M. J. M. Leask, and W. P. Wolf, J. Phys. Chem. Solids **23**, 1381 (1962).

¹² M. Kohgi, K. Iwasa, M. Nakajima, N. Metoki, S. Araki, N. Bernhoeft, J.-M. Mignot, A. Gukasov, H. Sato, Y. Aoki, and H. Sugawara, J. Phys. Soc. Jpn. **72**, 1002 (2003).

¹³ M. B. Maple, P.-C. Ho, V. S. Zapf, N. A. Frederick, E. D. Bauer, W. M. Yuhasz, F. M. Woodward, and J. W. Lynn, J. Phys. Soc. Jpn. Suppl. **71**, 23 (2002).

¹⁴ C. R. Rotundu and B. Andraka, in Low Temperature Physics: 24th International Conference on Low Temperature Physics, edited by Y. Takano, et al. (AIP Conference Proceedings, Melville, NY, 2006).